Available online at www.sciencedirect.com

ScienceDirect

Solar Energy 127 (2016) 269–284

SOLAR ENERGY

www.elsevier.com/locate/solener

Development of a new solar and geothermal based combined system for hydrogen production

Yusuf Bicer [a,*], Ibrahim Dincer [a,b]

[a] Clean Energy Research Laboratory (CERL), Faculty of Engineering and Applied Science, University of Ontario Institute of Technology, 2000 Simcoe Street North, Oshawa, Ontario L1H 7K4, Canada

[b] Department of Mechanical Engineering, King Fahd University of Petroleum and Minerals, Dhahran 31261, Saudi Arabia

Received 28 January 2015; received in revised form 6 December 2015; accepted 6 January 2016

Communicated by: Associate Editor S.A. Sherif

Abstract

A new combined system, using solar and geothermal resources, for hydrogen production, along with power generation, cooling and heating, is proposed and analyzed for practical applications. This combined renewable energy system consists of solar PV/T modules for heating, water heating and hydrogen production purposes and geothermal energy for electricity, cooling and hydrogen production. Energy and exergy analyses are conducted to assess the performance of the cycle, and the effects of various system parameters on energy and exergy efficiencies of the overall system and its subsystems are also studied. The overall energy and exergy efficiencies of the system can reach up to 10.8% and 46.3% respectively for a geothermal water temperature of 210 °C. Furthermore, the effects of varying geothermal water temperature and using different type of working fluids on the system performance are investigated.

Keywords: Solar energy; Geothermal energy; Hydrogen production; Exergy; Efficiency; Multigeneration

1. Introduction

As energy need in the world has increased rapidly within twenty-first century, developing suitable energy portfolio, especially for developing countries has become an important concern. In order to maintain stability of energy supply, use of various energy resources is emphasized. Therefore, multigeneration systems are considered one of the major alternatives for distributed energy production. However, renewable energy sources are not always available, due to the fluctuative nature, with a consequence of requiring energy storage or a hybrid system to balance these changes. When it is combined with the future energy carrier hydrogen production, it becomes a crucial renewable energy based multigeneration system. Using hydrogen in a fuel cell to produce electricity during low power generation or peak demand appears to be an alternative solution. The cost of hydrogen production from fossil fuels is dependent on fuels prices and carbon taxes, while the hydrogen produced from carbon-free sources is clearly independent of fuels prices and availability.

There has been a lot of research on renewable energy based multigeneration systems for hydrogen production. Al-Sulaiman et al. (2011) studied on exergy modeling to assess the exergetic performance of a novel tri-generation system using parabolic trough solar collectors (PTSC) and an organic Rankine cycle (ORC). In their system a single-effect absorption chiller is utilized to provide the

* Corresponding author.
E-mail addresses: yusuf.bicer@uoit.ca (Y. Bicer), ibrahim.dincer@uoit.ca (I. Dincer).

http://dx.doi.org/10.1016/j.solener.2016.01.031
0038-092X/

Nomenclature

C	compressor
$\dot{E}x$	exergy rate (kW)
ex	specific exergy (kJ/kg)
h	specific enthalpy (kJ/kg)
HX	heat exchanger
$\dot{m}$	mass flow rate (kg/s)
MW	molar mass (kg/kmol)
P	pressure (kPa)
$\dot{Q}$	heat rate (kW)
s	specific entropy (kJ/kg K)
T	temperature (°C or K)
$\dot{W}$	work rate (kW)
HHV	higher heating value
LiBr	lithium bromide
PTSC	parabolic trough solar collectors
PV/T	photovoltaic/thermal
COP	coefficient of performance

Greek letters

η_{en}	energy efficiency
η_{ex}	exergy efficiency

Subscripts and superscripts

abs	absorption
in	inlet of a component
out	outlet of a component
0	ambient condition
i	state number
C	compressor
cond	condenser
d	destruction
Eva	evaporator
GEN	generator
ORC	organic Rankine cycle
s	source or sink
P	pump
TES	thermal energy storage
pce	power conversion efficiency
HX	heat exchanger
HP	heat pump
EV	expansion valve
T	turbine
ph	physical
ch	chemical
ov	overall
sys	system
sc	short circuit
oc	open circuit
mp	nominal
m	maximum
AC	absorption cooling
PV	photovoltaic
geo	geothermal
elec	electrolysis
E	electrolyzer
1, 2, … i	state points

necessary cooling energy and a heat exchanger is utilized to provide the necessary heating energy. Ozturk and Dincer (2013a) studied a solar-based multigeneration system and found its exergy efficiency to be around 57%. Ozturk and Dincer (2013b) indicated that the integration of various systems, multigeneration for multiple purposes increases energy and exergy efficiencies. Dincer and Zamfirescu (2011) showed that renewable energy-based multigeneration system decreases fuel prices and harmful pollutant emissions, compared to conventional systems. Khalid et al. (2015) proposed a biomass and solar integrated based system for multigeneration for power, cooling, hot water, heated air and found the overall system exergy efficiency as 39.7%. Karellas and Braimakis (2016) analyzed a micro-scale trigeneration system capable of combined heat and power production and refrigeration using R245fa organic medium. The exergy efficiency of the ORC was estimated at about 7%. They also assessed the system economically for a particular apartment block in Greek island with a payback period of 7 years.

Suleman et al. (2014) designed a solar and geothermal energy based system for multigeneration applications. They used two organic Rankine cycles for power generation, an absorption chiller cycle for cooling production and a drying system to dry wet products. Ayub et al. (2015) conducted thermos economic analysis of a combined solar geothermal plant. Solar system contribution to the system power output is limited to 7%. Comparing solely solar or geothermal systems, the constant-flow solar trough system suggests 5.5% and the variable-flow solar trough system gives 6.3% higher power output compared to the sole geothermal system. Ozcan and Dincer (2014) conducted analysis and performance assessment of a solar driven hydrogen production plant running on an Mg–Cl cycle through energy and exergy methods by energy and exergy efficiencies of 18.8% and 19.9%, respectively. Ahmadi et al. (2013) proposed a multi-generation system based on a biomass combustor, an organic Rankine cycle (ORC), an absorption chiller and a proton exchange membrane electrolyzer to produce hydrogen, and a domestic water heater for hot water production. Wang et al. (2010) evaluated a low temperature ORC with a working fluid of R245fa. They found the overall power generation efficiency as 4.2%, when the evacuated solar collector is utilized. Their results emphasized that using R245fa as working fluid in the low-temperature solar power Rankine cycle system is feasible and the performance is acceptable. Cho et al. (2014) reviewed different methods of CHP system analysis

by explaining possible advantages of multigeneration systems such as additional options for energy outputs, providing increased opportunities to minimize primary energy consumption and maximizing exergy efficiency. Zhang and Lior (2006) analyzed a cogeneration system consisting of ammonia–water Rankine cycle and an ammonia refrigeration cycle for refrigeration and power output. They found cycle energy and exergy efficiencies as 27.7% and 55.7%, respectively. Their exergy analysis indicated that conventional enhancements in the condenser, heat exchangers and turbine efficiency can increase the cycle exergy efficiency to 60%. Kumar and Kumar (2014) studied integrated power generation and waste heat operated absorption, ejector-jet pump refrigeration cycle. The refrigerants used in the cycle have no ozone depletion potential and negligible global-warming potential. The percentage of exergy destruction was highest in the condenser-1 and HRSG unit.

El-Emam and Dincer (2013) studied on thermodynamic and economic analyses of a geothermal regenerative organic Rankine cycle based on both energy and exergy concepts. The energy and exergy efficiency values are found to be 16.37% and 48.8%, respectively. The mass flow rates of the organic fluid, cooling water and provided geothermal water are calculated for a net out power of 5 MWe. AlZaharani et al. (2013) proposed an integrated system which is comprised of a supercritical carbon dioxide (CO_2) Rankine cycle cascaded by an Organic (R600) Rankine cycle, an electrolyzer, and a heat recovery system. It is designed to utilize a medium-to-high temperature geothermal energy source for power and hydrogen production, and thermal energy utilization for space heating. The system provides overall energy and exergy efficiencies of 13.67% and 32.27%, respectively. Balta et al. (2010) researched for geothermal-based hydrogen production methods, and their technologies and application possibilities. They used a high-temperature electrolysis (HTE) process coupled with and powered by a geothermal source. Balta et al. (2009) discussed the potential methods for geothermal-based hydrogen production by stating electrolytic hydrogen production yields the highest purity hydrogen. Hand (2008) studied hydrogen production using geothermal energy by making simulation studies for different type of geothermal water temperatures. He has indicated in his research that it can be shown using first and second laws of thermodynamics that energy can be added through heat water input to improve the electrolyzer efficiency. He showed that there is a 17% increase in efficiency by increasing the temperature from 20 °C to 80 °C. Yekoladio et al. (2015) studied thermodynamic analysis and performance optimization of geothermal power cycles. Their binary-cycles are operating in the range of moderately low temperature and liquid-dominated geothermal resources with temperatures of 110 °C to 160 °C. They concluded that regenerative ORCs require organic fluids with lower vapor specific heat capacity for an optimal operation of the binary-cycle where isobutane is one of the key options.

Yilanci et al. (2009) studied solar hydrogen production methods and their current status. They discussed solar-hydrogen/fuel cell hybrid energy systems for stationary applications and performed preliminary energy and exergy efficiency analyses for a photovoltaic-hydrogen/fuel cell hybrid energy system. Kalogirou et al. (2016) summarized exergy analysis of solar thermal systems realized in last two years concluding such that solar energy can be used in the collection or storage of thermal energy, drying, heating cooling and multigeneration, hydrogen production, hybrid systems, solar ponds, electricity generation systems and desalination. Sahin et al. (2007) defined a new efficiency which is useful in studying PV performance and possible improvements. They found that exergy efficiencies, which incorporate the second law of thermodynamics and account for solar irradiation exergy values, are lower than energy efficiencies ranging from 2% to 8%. Joshi et al. (2009) investigated exergy efficiency for PV and PV/T systems that is useful in studying the PV and PV/T performances. In their experimental data of New Delhi, it is found that the energy efficiency varies from a minimum of 33% to a maximum of 45%, the corresponding exergy efficiency varies from a minimum of 11.3% to a maximum of 16% for PV/T systems. Ratlamwala et al. (2011) proposed an integrated PV/T absorption system for cooling and hydrogen production in U.A.E. Bouzguenda (2012) studied performance analysis software of hybrid systems including wind turbines, solar systems, and storage batteries backed up with diesel generators using HOMER for different locations in Oman. He concluded that hybrid systems offer many advantages such as reducing diesel operating time, fuel consumption, and maintenance.

Future's energy carrier hydrogen can be produced in many different ways. Water electrolysis currently provides an attractive solution to the problem of hydrogen production. One of the critical benefits which water electrolysis has over other technologies for production of hydrogen is that it is compatible with both recent technologies and future technologies such as solar, wind, wave and geothermal. Another advantage of using water electrolysis is that it can provide onsite hydrogen. Requiring electrical energy for water electrolysis, in order to produce hydrogen in an environmental friendly manner, we need to use carbon free renewable energy sources. Solar and geothermal energy represent a great potential to be the power source of multigeneration systems including electrolysis. In electrolysis process, the electrolyzer is utilized to break the water molecule bond. As the water molecule breaks, it splits into hydrogen and oxygen. The hydrogen molecules are then taken out of the electrolyzer and are stored in a tank. Dincer (2012) defined the green hydrogen production methods and assessed these processes for comparison purposes. Various case studies are presented to highlight the importance of green hydrogen production methods and systems for practical applications. Acar and Dincer (2014) presented a comparative environmental impact assessment of possible hydrogen production methods from

renewable and non-renewable sources and compared the performances of hydrogen production methods and assess their economic, social and environmental impacts. Carmo et al. (2013) prepared a review in which PEM water electrolysis is comprehensively highlighted and discussed. The technical state and the progress in the areas of electrocatalysis, essential components, and modeling activities for PEM water electrolysis are inspected in the review. Ferrero et al. (2013) worked on comparative analysis between low- and high-temperature electrolysis for hydrogen generation. The comparison is carried out with two electrolysis systems generating hydrogen at the same production rate and pressure. Barbir (2005) addressed specific issues regarding the use of PEM electrolyzer in the renewable energy systems such as sizing of electrolyzer, intermittent operation, output pressure, oxygen generation, water consumption and efficiency. They determined the economics of PV-hydrogen not only by the cost of the PV array and the electrolyzer, but also by the capacity factor and the electrolyzer efficiency. Guo et al. (2011) studied theoretical analyses of natural and conventional working fluids based Rankine cycles run by low-temperature geothermal resources. They used the method of pinch point analysis by computer models. They concluded that R125 proposes better performances thermodynamically and techno-economically. Tunc et al. (2013) analyzed Kizildere Geothermal power plant in terms of exergy by using organic Rankine cycle. The results of their study showed that the cycle efficiency can vary between 8% and 30% based on the working fluid used. Solar energy is clean, sustainable and cost effective source of energy. However, there is one disadvantage of solar energy which is being intermittent. In the current study, in order to eliminate this deficiency, geothermal energy, which is continuous and renewable, is utilized by integrating an organic Rankine cycle. Furthermore, producing hydrogen using both renewable resources, solar energy can be stored in the form of chemical fuel. The advantages and cost analyses of combining solar and geothermal energy system were studied in the literature by Astolfi et al. (2011) as they concluded that the solar-geothermal hybrid concept could represent a good opportunity for lower cost electricity production. Furthermore, one of the earlier studies from our group (Suleman et al., 2014) confirmed that combining solar and geothermal subsystems brings up some advantages, such offsetting the mismatch between demand and supply, reducing life cycle emissions, reducing life cycle costing and increasing efficiencies.

In this paper, a new multigeneration system based on carbon free renewable energy sources for power generation, hydrogen production, cooling and heating is developed and analyzed. The developed system consists of already proven and mature technologies which increases the practicality of the system. The system differs from many multigeneration systems in terms of zero fossil resources usage and zero carbon emissions by using two different renewable energy sources. Combining thermal energy storage, PV/T systems and heat pump system brings a special and distinctive cycle with higher exergetic efficiency. Compared to CHP systems, having cooling and hydrogen production is a significant advantageous for which we can utilize in many industrial applications as alternative fuel. The particular objectives of this paper are to develop and to assess a new integrated multigeneration system using geothermal and solar energy by using energy and exergy analyses, including the determination of overall energy and exergy efficiencies of the multigeneration system and its subsystems; and to execute a parametric study to determine the effects of various parameters on the overall energy and exergy efficiencies of the multigeneration system and its subsystems.

2. System description

While designing a system, there are three important aspects; resources, system and application (Dincer and Zamfirescu, 2012). In the designed multi-generation system, there are two type of renewable energy resources; solar thermal/photovoltaic and geothermal energy. The system consists of an organic Rankine cycle, heat pump, absorption cooling system, thermal energy storage and hydrogen production system. Application is the purpose of the system. The designed multi-generation system serves for hydrogen production, heating, cooling and power generation for consumers which are located on a geothermal area. High temperature geothermal resources range between 150 and 350 °C for many regions in the world (Tunc et al., 2013; Coskun et al., 2012; Bertani, 2012; Chamorro et al., 2012). Following geothermal regions can be listed as possible application areas; Innamincka-Australia (250 °C), South Meager-Canada (220–275 °C), Yangbajain-China (250–330 °C), Ahuachapán-El Salvador (250 °C), Bedugul-Indonesia (280–320 °C), Larderello-Italy (300–350 °C) Bertani, 2012. The proposed system can be appropriately applicable to any geothermal area satisfying the temperature and solar irradiance limit such as Denizli-Turkey (Tunc et al., 2013). Average sunshine duration of Denizli is 4.3 h in February and 11.6 h in July while the average temperature during the seasons vary between 6 °C and 28 °C. Yearly irradiation is around 1650 kW h/m^2-year (Turkish State Meteorological Service). As system schematic is shown in Fig. 1, organic Rankine cycle whose working fluid is isobutane is run by a medium-high temperature geothermal water by giving its heat to evaporator of organic Rankine cycle. The inlet temperature of Evaporator 1 is 201 °C and outlet temperature is 150 °C which is utilized by Heat Exchanger 1 for heating the water in electrolysis. The inlet temperature of turbine with a nominal power of 1.85 MW is 145 °C and steam leaves the turbine with 100 °C which transfers its heat to generator of absorption cooling system. This temperature is satisfactory for a LiBr-water based absorption cooling system. The turbine is coupled with a power generator to supply the required electricity for electrolysis of water. Condensers of the

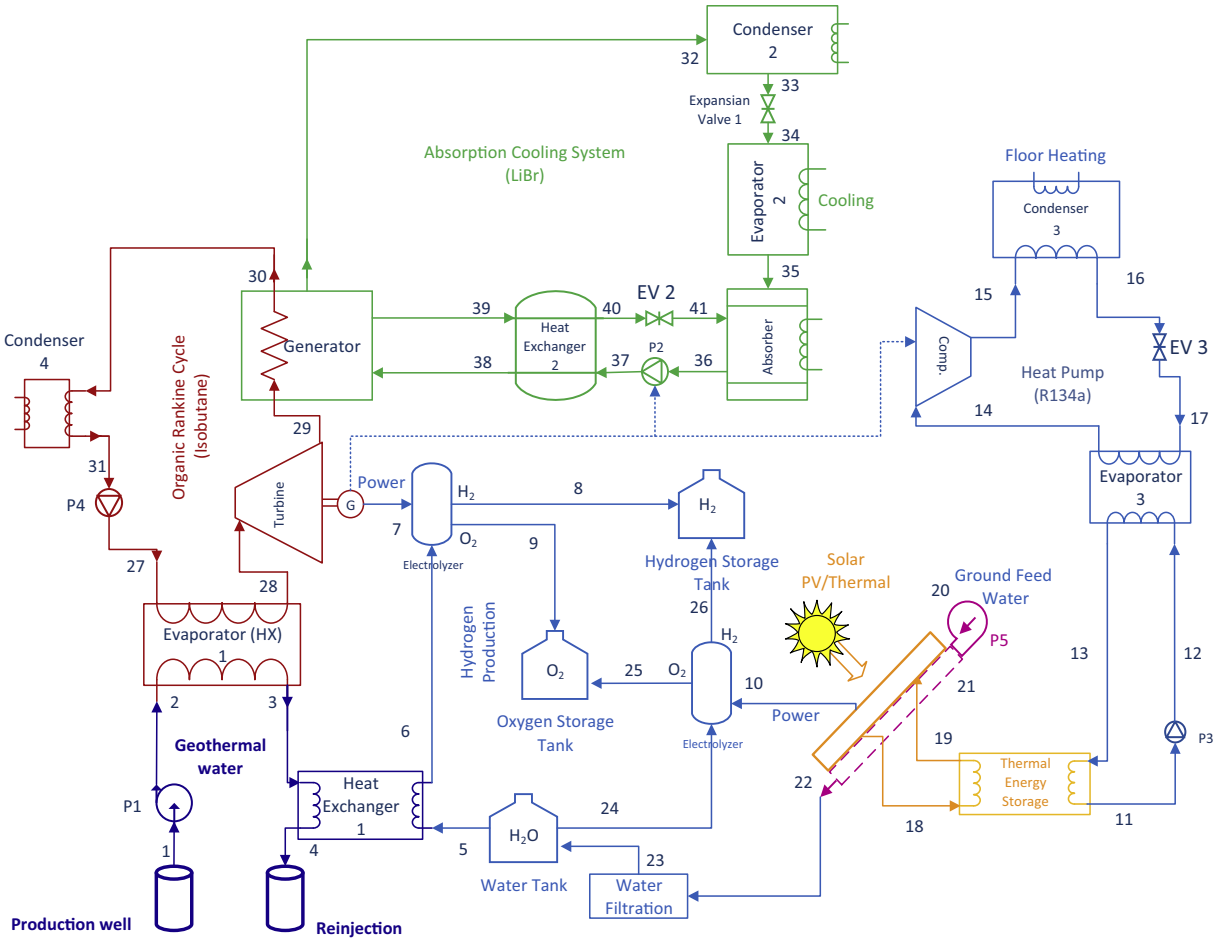

Fig. 1. Schematic diagram of designed multigeneration system.

system are cooled by a cold ground water which is supplied through the pump. This ground water is also the water supply of electrolysis process after filtration. The temperature of ground water is around 10 °C. For PV based hydrogen production, the ground water is heated through a duct system under the PV/T modules to increase the electrolysis efficiency. Obtained cooling effect in the outlet of Evaporator 2 of absorption cooling system is used to cool the residential buildings. In order to heat the residential buildings, a heat pump with a working fluid of refrigerant R134a is used. The energy supply of heat pump is stored heat in thermal energy storage system with a capacity of 15 kW at a temperature of 60 °C. Refrigerant R134a is chosen to enable low temperature application. The water for electrolysis is filtered and stored in water tank. Obtained oxygen from electrolysis is also stored in oxygen tank for later medical purposes. Working fluid refrigerant R134a leaves Evaporator 3 with a temperature of 9.5 °C. After compression, it enters to Condenser 3 with 75 °C and leaves at 35 °C. The heat output of Condenser 3 is utilized for residential heating purposes. Solar thermal system reaches up to 85 °C and the hot water is stored in thermal energy storage to have 24 h operation of heat pump with a capacity of 20 kW. Since system is applied on a residential area, heating, cooling and electricity are always needed in 24 h a day, 7 days a week. By using geothermal energy source and thermal energy storage system, it is enabled to have an uninterrupted power generation, heating, cooling and hot water. The required electricity for whole processes is

Table 1
PV/T module specifications and important analysis data of solar system (modified from VOLTHER PowerTherm&PowerVolt (2014)).

Dimensions (mm)	1310 × 2175 × 180
Gross area (m^2)	2.85
Weight (kg)	34.4
Absorber panel	Mono-Crystalline
Number of cells	72
Cell dimensions (mm)	125 × 125
W_{Power} (W) nominal power	235
I_{mp} (A) nominal current	5.98
I_{sc} (V) short circuit current	6.4
V_{mp} (V) nominal voltage	39.36
V_{oc} (V) open circuit voltage	44.64
Flow (l/h)	360
Maximum temperature (°C)	<134
Cell temperature (T_{cell})	75 °C
Sun temperature (T_{sun})	5504.85 °C
PV/T modules total area (A)	85 m^2
Direct normal irradiation (S_T)	770 W/m^2

supplied by generated electricity in the organic Rankine cycle. Generated electricity in the PV/T modules is used in electricity consumption of Pump 5 and 1 which is used in water pumping from ground source and in pumping to heat pump system, respectively. The generator coupled with turbine is connected to the grid in order to work parallel with the grid. 30 PV/T modules, whose features are given in Table 1, are used in the designed system which corresponds to 7 kW installed solar power (VOLTHER PowerTherm&PowerVolt, 2014).

3. Thermodynamic analysis

Energy and exergy analyses are performed for the proposed multigeneration system, in order to provide the information about its performance, efficiency and exergy destructions. The assumptions made for the analysis of the integrated system are listed as follows:

- The expansion valves, compressors, pumps and turbine are adiabatic.
- Air, hydrogen and oxygen are treated as ideal gas.
- The ambient has a temperature $T_0 = 25\ ^\circ C$ and a pressure $P_0 = 100$ kPa
- The changes in kinetic and potential energy and exergy terms are negligible.
- The processes taking place are steady state and steady flow.
- There is no chemical reaction taking place between the refrigerant and absorbent. Therefore, chemical exergy is neglected and only physical exergy is taken into account.
- The working fluid of organic Rankine cycle is isobutane.
- The working fluid of heat pump is R134a.
- The working fluid of absorption cooling system is LiBr–Water.
- The solar PV/T back surface temperature is taken to be 75 °C.
- The chemical reactants and products are at the reaction temperature and a pressure of 1 atm.

The energy balance, based on the first law of thermodynamics, is applied to each of the sub system components. The general steady state form of the energy balance equation for any component can be written as follows:

$$\dot{Q} - \dot{W} + \sum \dot{m}_{in} h_{in} - \sum \dot{m}_{out} h_{out} = 0 \tag{1}$$

where $\dot{Q}$ and $\dot{W}$ represent the heat transfer and work crossing the component boundaries and $\dot{m}$ and h represent the mass flow rate and the specific enthalpy of the streams of the system working fluid.

Analysing only in terms of first law of thermodynamics prevents designing accurate systems. Hence, exergy analysis is one of the most important aspects for the design and analysis of thermal systems. It is based on the second law of thermodynamics. Exergy is a measure of the system state departure from the environment state and is considered also as a measure of the available energy (Cengel and Boles, 2014).

The flow exergy terms for each state point are defined as following formula;

$$ex_i = h_i - h_0 - T_0(s_i - s_0) \tag{2}$$

Applying the exergy balance on the system components at steady state, the exergy destruction in each component can be calculated as follows:

$$\dot{E}x_{d_i} = \dot{E}x^{Q_i} - \dot{E}x_{W_i} + \sum \dot{m}_{in} ex_{in} - \sum \dot{m}_{out} ex_{out} \tag{3}$$

where $\dot{E}x_{d_i}$ represents the exergy destruction rate that occurs at the device i, $\dot{E}x_{W_i}$ and $\dot{E}x^{Q_i}$ represent the exergy rate due to work and heat transfer respectively across the system boundaries and the ex_{in}, ex_{out} represents the exergy rate carried with the flow in and out from the system. The exergy transfer due to heat can be expressed as follows:

$$\dot{E}x^{Q_i} = \dot{Q}_i \left(1 - \frac{T_0}{T_{s_i}}\right) \tag{4}$$

where T_0 is the ambient temperature that describes the state at which the system is in unrestricted equilibrium with the environment and it cannot undergo any state change through any kind of interaction with the environment (Dincer and Rosen, 2013) and T_S is the temperature of source in case there is a heat penetration and temperature of sink in case there is a heat loss.

The exergy destruction rate is calculated by multiplication of ambient temperature with entropy generation in each component:

$$\dot{E}x_{d_i} = \dot{T}_0 \cdot \dot{S}_{gen,i} \tag{5}$$

where $\dot{S}_{gen,i}$ denotes the entropy generation rate in the component i and it is determined by applying the entropy balance equation for a steady state operation on each component of the system as follows:

$$\dot{S}_{gen,i} = \sum \dot{m}_{out} s_{out} - \sum \dot{m}_{in} s_{in} - \sum \left(\frac{\dot{Q}}{T}\right) \tag{6}$$

Here, the exergy associated with a process at a specified state is the sum of two contributions: physical and chemical.

Thus, the specific exergy of the hydrogen production process is calculated by:

$$ex_i = h_i - h_0 - T_0(s_i - s_0) + ex_{ch} \tag{7}$$

The chemical exergy based on a typical exergy reference environment exhibiting standard values of the environmental temperature T_0 and pressure P_0 such as 25 °C and 100 kPa is named standard chemical exergy. The data of the chemical exergies for the reactants and products are utilized from the literature (Moran et al., 2011).

The electrolysis reaction is the opposite of the formation of water reaction:

$$H_2O + \text{Electrical Energy} = H_2 + \frac{1}{2}O_2 \tag{8}$$

The exergy content of produced hydrogen is calculated as follows:

$$\dot{E}x_{H_2} = \dot{m}_{H_2}(ex_{H_2,ch} + ex_{H_2,ph}) \tag{9}$$

where

$$ex_{H_2,ch} = \frac{236.1 * 1000}{MW_{H_2}} \tag{10}$$

where 236.1 kJ/g mole is taken to be exergy content of hydrogen (The Exergoecology Portal) and MW_{H_2} is the molar mass of hydrogen in kg/kmol.

The efficiency of electrolyzer is taken to be 70% and 65% (Roy et al., 2006; Nieminen et al., 2010; Artuso et al., 2011) for PV and Geothermal, respectively as per following formula:

$$\eta_{electrolyzer} = \frac{m_{H_2} * HHV}{\dot{W}_{electrolyzer}} \tag{11}$$

where $\dot{W}_{electrolyzer}$ is taken to be 50% of turbine work output for geothermal system and 85% of PV/T work output for solar based hydrogen production. HHV represents the higher heating value of hydrogen.

The electrolysis efficiency of geothermal based hydrogen production is:

$$\eta_{en,elect,Geo} = \frac{m_{H_2} * h_{H_2} + m_{O_2} * h_{O_2}}{\dot{W}_{out,T}} \tag{12}$$

The exergy efficiency of electrolysis process is the ratio of the exergy of the reactants (water), over the power input which can be determined by the following formula:

$$\eta_{ex,elec,Geo} = \frac{m_{H_2} * ex_{H_2} + m_{O_2} * ex_{O_2}}{\dot{W}_{out,T}} \tag{13}$$

The electrolysis efficiency of PV/T based hydrogen production is:

$$\eta_{en,elec,PV/T} = \frac{m_{H_2} * h_{H_2} + m_{O_2} * h_{O_2}}{\dot{W}_{PV}} \tag{14}$$

and the exergy efficiency becomes

$$\eta_{ex,elec,PV/T} = \frac{m_{H_2} * ex_{H_2} + m_{O_2} * ex_{O_2}}{\dot{W}_{PV}} \tag{15}$$

All of the important subsystem exergy balance equations and exergy efficiency definitions are given in Table 3. The exergy efficiency of a process can be given as the ratio of exergy output that is produced by the system to the total exergy input. The exergy efficiencies for the sub-systems can be stated as follows:

The organic Rankine cycle exergy efficiency is the ratio of net work generated by turbine over total exergy input:

$$\eta_{ex,ORC} = \frac{\dot{W}_{out,T} - \dot{W}_{in,P4}}{(\dot{m}_2 ex_2 - \dot{m}_3 ex_3)} \tag{16}$$

The absorption cooling system energetic and exergetic COP are as follows:

$$COP_{en,AC} = \frac{\dot{Q}_{AC}}{(\dot{m}_{29}h_{29} - \dot{m}_{30}h_{30})} \tag{17}$$

where $\dot{Q}_{AC}$ is heat absorbed by Evaporator 2.

The COP reversible can be found as follows:

$$COP_{reversible} = \left(\frac{T_{32} - T_0}{T_{32} + 273}\right)\left(\frac{10 + 273}{T_0 - 10}\right) \tag{18}$$

The exergetic COP of absorption cooling system is the ratio of energetic COP over reversible COP stated as:

$$COP_{ex,AC} = \frac{COP_{en,AC}}{COP_{reversible}} \tag{19}$$

In the heat pump system, useful output is the heat out from Condenser 3. Therefore, both energetic and exergetic COPs of heat pump system can be written as

$$COP_{en,HP} = \frac{\dot{Q}_{out,Cond3}}{\dot{W}_{in,C}} \tag{20}$$

$$COP_{ex,HP} = \frac{\dot{Q}_{out,Cond3}\left(1 - \frac{T_0}{T_s}\right)}{\dot{W}_{in,C}} \tag{21}$$

By considering all useful outputs and total inputs, overall system energy and exergy efficiencies are defined as follows:

$$\eta_{en,ov,sys} = \frac{\dot{W}_{out,T} * 0.5 + \dot{W}_{PV} * 0.15 - \sum \dot{W}_{Pumps} - \dot{W}_{in,C} + \dot{m}_{26}h_{26} + \dot{m}_{25}h_{25} + \dot{m}_9 h_9 + \dot{m}_8 h_8 + \dot{Q}_{out,Cond3} + \dot{Q}_{AC}}{\dot{m}_1 h_1 + \dot{Q}_{Solar}} \tag{22}$$

$$\eta_{ex,ov,sys} = \frac{\dot{W}_{out,T} * 0.5 + \dot{W}_{PV} * 0.15 - \sum \dot{W}_{Pumps} - \dot{W}_{in,C} + \dot{m}_{26}ex_{26} + \dot{m}_{25}ex_{25} + \dot{m}_9 ex_9 + \dot{m}_8 ex_8 + \dot{E}x^{\dot{Q}_{Cond3}} + \dot{E}x^{\dot{Q}_{AC}}}{\dot{m}_1 ex_1 + \dot{E}x^{\dot{Q}_{Solar}}} \tag{23}$$

4. Results and discussion

In energy and exergy analyses of the designed renewable energy based integrated multigeneration system, values of mass flow rate (kg/s), temperature (°C), pressure (kPa), specific enthalpy (kJ/kg) and specific exergy (kJ/kg) are determined for the each state of the system as listed in

Table 2
Process data for the multigeneration system.

State no	Fluid/gas type	T (°C)	P (kPa)	$\dot{m}$ (kg/s)	h (kJ/kg)	s (kJ/kg K)	ex (kJ/kg)
0	Water	25	100	–	104.8	0.3669	–
0′	R134a	25	100	–	276.4	1.106	–
0″	LiBr–Water	25	100	–	50.78	0.1773	–
0‴	Isobutane	25	100	–	599	2.515	–
1	Water	200	2500	45	852.8	2.329	162.9
2	Water	201	2600	45	857.3	2.339	164.6
3	Water	150	2600	45	633.6	1.84	89.68
4	Water	90	2600	45	378.9	1.191	28.44
5	Water	40	200	0.01	167.7	0.5722	1.627
6	Water	80	200	0.01	335	1.075	542.8
7	–	25	100				
8	Hydrogen	80	150	0.005032	791.4	65.58	117,672
9	Oxygen	80	150	0.004968	50.68	6.461	159.7
10	–	25	100				
11	Water	60	180	0.035	251.3	0.8311	8.053
12	Water	63	200	0.035	263.9	0.8686	9.441
13	Water	10	190	0.035	42.17	0.1509	1.724
14	R134a	9.5	300	0.04	258.7	0.9595	26.06
15	R134a	75	950	0.04	309.8	1.037	54.06
16	R134a	35	950	0.04	100.9	0.3712	43.57
17	R134a	2	300	0.04	100.9	0.4362	24.2
18	Water	85	150	0.1	356	1.134	22.38
19	Water	65	150	0.1	272.2	0.8934	10.36
20	Water	10	120	0.02	42.1	0.151	1.654
21	Water	12	200	0.02	50.55	0.1804	1.322
22	Water	43	200	0.02	180.2	0.6121	2.285
23	Water	43	200	0.02	180.2	0.6121	2.285
24	Water	40	200	0.01	167.7	0.5722	525.4
25	Oxygen	40	150	0.009967	13.74	6.35	155.8
26	Hydrogen	40	150	0.00003293	215.4	63.85	117,612
27	Isobutane	77	1500	25	396.9	1.624	63.65
28	Isobutane	145	1500	25	807.4	2.74	141.5
29	Isobutane	100	300	25	734	2.766	60.37
30	Isobutane	85	300	25	703.6	2.683	54.76
31	Isobutane	75	300	25	391.4	1.61	62.32
32	Water	90	5.48	0.18	2669	8.674	86.85
33	Water	40	5.48	0.18	167.5	0.5723	1.434
34	Water	5	0.8	0.18	40.73	0.1475	1.319
35	Water	5	0.8	0.18	2510	9.064	88.1
36	LiBr–Water	35	0.8	1.9	88.12	0.2075	28.32
37	LiBr–Water	38	5.48	1.9	94.09	0.2269	28.53
38	LiBr–Water	53	5.48	1.9	124.2	0.3217	30.39
39	LiBr–Water	90	5.48	2	229.1	0.4861	86.2
40	LiBr–Water	60	5.48	1.72	173.8	0.3271	78.35
41	LiBr–Water	55	0.8	1.72	164.7	0.2996	77.48

Table 2. The reference conditions are taken to be the ambient conditions. Thermodynamic values are calculated using Engineering Equation Solver (EES) software which is a powerful software for thermodynamic analysis.

Solar PV/T modules are capable of both generating hot water and electricity. Selected PV/T module has a nominal power of 235 W. The exergy destruction values, energy consumption or generation values, energy and exergy efficiency values of important components are listed in Table 4. As seen in Fig. 2, highest exergy destruction rates are observed in Heat Exchanger 1, geothermal based electrolysis process and Evaporator 1. Because Heat Exchanger 1 and Evaporator 1 content high amount of mass flow rate as geothermal water input. The exergy destruction rates of Pump 1 and Turbine are 124.9 kW and 193.1 kW respectively as seen in Table 4 and Fig. 2. Absorber has also an exergy destruction rate of 113.3 kW which is followed by Pump 4 with 105.4 kW. Highest exergy efficiency values are observed in Expansion Valve 1 and 2, as 92% and 99% respectively. Exergy efficiencies of Generator and Evaporator 2 are 93% and 95% respectively. In organic Rankine cycle, the turbine generates approximately 1.8 MW power with an exergy efficiency of 90%. The turbine exergy destruction rate is 193.1 kW. The thermal energy storage energy and exergy efficiencies are 87% and 18% respectively. The exergy efficiency is lower than energy efficiency, therefore while designing the thermal energy storage systems, exergy ethically analyses are suggested to be

Table 3
Exergy destruction rates and exergy efficiency equations for the system components.

Component	Exergy destruction rate definition	Exergy efficiency definition
Turbine	$\dot{E}x_{d,T} = \dot{m}_{28}ex_{28} - \dot{m}_{29}ex_{29} + \dot{W}_{out,T}$	$\eta_{ex,T} = \frac{\dot{W}_{out,T}}{(\dot{m}_{28}ex_{28} - \dot{m}_{29}ex_{29})}$
Condenser 4	$\dot{E}x_{d,Cond4} = \dot{m}_{30}ex_{30} - \dot{m}_{31}ex_{31} + \dot{Q}_{out,Cond4}\left(1 - \frac{T_0}{T_s}\right)$	$\eta_{ex,Cond4} = \frac{\dot{Q}_{out,Cond4}\left(1-\frac{T_0}{T_s}\right)}{(\dot{m}_{30}ex_{30} - \dot{m}_{31}ex_{31})}$
Pump 4	$\dot{E}x_{d,P4} = \dot{m}_{31}ex_{31} + \dot{W}_{in,P4} - \dot{m}_{27}ex_{27}$	$\eta_{ex,P4} = \frac{(\dot{m}_{27}ex_{27} - \dot{m}_{31}ex_{31})}{\dot{W}_{in,P4}}$
Evaporator 1	$\dot{E}x_{d,Eva1} = \dot{m}_{27}ex_{27} + \dot{m}_{2}ex_{2} - \dot{m}_{28}ex_{28} - \dot{m}_{3}ex_{3}$	$\eta_{ex,Eva1} = \frac{(\dot{m}_{28}ex_{28} - \dot{m}_{27}ex_{27})}{(\dot{m}_{2}ex_{2} - \dot{m}_{3}ex_{3})}$
Generator	$\dot{E}x_{d,GEN} = \dot{m}_{38}ex_{38} + \dot{m}_{29}ex_{29} - \dot{m}_{30}ex_{30} - \dot{m}_{39}ex_{39} - \dot{m}_{32}ex_{32}$	$\eta_{ex,GEN} = \frac{(\dot{m}_{32}ex_{32} + \dot{m}_{39}ex_{39} - \dot{m}_{38}ex_{38})}{(\dot{m}_{29}ex_{29} - \dot{m}_{30}ex_{30})}$
Condenser 2	$\dot{E}x_{d,Cond2} = \dot{m}_{32}ex_{32} - \dot{m}_{33}ex_{33} - \dot{Q}_{out,Cond2}\left(\left\|1 - \frac{T_0}{T_s}\right\|\right)$	$\eta_{ex,Cond2} = \frac{\dot{Q}_{out,Cond2}\left(\left\|1-\frac{T_0}{T_s}\right\|\right)}{(\dot{m}_{32}ex_{32} - \dot{m}_{33}ex_{33})}$
Evaporator 2	$\dot{E}x_{d,Eva2} = \dot{m}_{34}ex_{34} + \dot{Q}_{AC}\left(\left\|1 - \frac{T_0}{T_{35}}\right\|\right) - \dot{m}_{35}ex_{35}$	$\eta_{ex,Eva2} = \frac{\dot{Q}_{AC}\left(\left\|1-\frac{T_0}{T_{35}}\right\|\right)}{(\dot{m}_{35}ex_{35} - \dot{m}_{34}ex_{34})}$
Heat exchanger 2	$\dot{E}x_{d,HX2} = \dot{m}_{39}ex_{39} + \dot{m}_{37}ex_{37} - \dot{m}_{40}ex_{40} - \dot{m}_{38}ex_{38}$	$\eta_{ex,HX2} = \frac{(\dot{m}_{38}ex_{38} - \dot{m}_{37}ex_{37})}{(\dot{m}_{39}ex_{39} - \dot{m}_{40}ex_{40})}$
Solar PV/T	$\dot{E}x_{d,Solar} = \dot{m}_{19}ex_{19} + \dot{Q}_{in,Solar}\left(1 - \frac{T_0}{T_{sun}}\right) - \dot{m}_{18}ex_{18} - \dot{W}_{PV}$	$\eta_{ex,Solar} = \frac{\dot{W}_{PV} + \dot{m}_{18}ex_{18} - \dot{m}_{19}ex_{19}}{S_T\left(1-\frac{T_0}{T_{sun}}\right)\frac{A}{1000}}$
Geothermal based electrolysis	$\dot{E}x_{d,E,Geo} = \dot{m}_{6}ex_{6} + \dot{W}_{out,T} - \dot{m}_{8}ex_{8} - \dot{m}_{9}ex_{9} - \dot{Q}_{loss,E,Geo}\left(1 - \frac{T_0}{T_8}\right)$	$\eta_{ex,elec,Geo} = \frac{(\dot{m}_{8}ex_{8} + \dot{m}_{9}ex_{9})}{\dot{W}_{out,T}}$
PV/T based electrolysis	$\dot{E}x_{d,E,PV} = \dot{m}_{24}ex_{24} + \dot{W}_{PV} - \dot{m}_{26}ex_{26} - \dot{m}_{25}ex_{25} - \dot{Q}_{loss,E,PV}\left(1 - \frac{T_0}{T_s}\right)$	$\eta_{ex,elec,PV} = \frac{(\dot{m}_{26}ex_{26} + \dot{m}_{25}ex_{25})}{\dot{W}_{PV}}$
Compressor	$\dot{E}x_{d,C} = \dot{m}_{14}ex_{14} + \dot{W}_{in,C} - \dot{m}_{15}ex_{15}$	$\eta_{ex,C} = \frac{(\dot{m}_{15}ex_{15} - \dot{m}_{14}ex_{14})}{\dot{W}_{in,C}}$
Condenser 3	$\dot{E}x_{d,Cond3} = \dot{m}_{15}ex_{15} - \dot{m}_{16}ex_{16} - \dot{Q}_{out,Cond3}\left(\left\|1 - \frac{T_0}{T_s}\right\|\right)$	$\eta_{ex,Cond3} = \frac{\dot{Q}_{out,Cond3}\left(\left\|1-\frac{T_0}{T_s}\right\|\right)}{(\dot{m}_{15}ex_{15} - \dot{m}_{16}ex_{16})}$
Evaporator 3	$\dot{E}x_{d,Eva3} = \dot{m}_{17}ex_{17} + \dot{m}_{12}ex_{12} - \dot{m}_{14}ex_{14} - \dot{m}_{13}ex_{13}$	$\eta_{ex,Eva3} = \frac{\dot{m}_{14}ex_{14} - \dot{m}_{17}ex_{17}}{\dot{m}_{12}ex_{12} - \dot{m}_{13}ex_{13}}$

Table 4
Thermodynamic analysis data of the multi-generation system components.

Component	Exergy destruction rate (kW)	Exergy efficiency (%)	Power or heat transfer rate (kW)
Condenser 2	2.962	81	450.2
Condenser 3	0.368	12	8.357
Condenser 4	81.93	70	7806
Heat exchanger 1	2750	1	11,461
Heat exchanger 2	34.09	9	–
Electrolysis geothermal	961.4	32	1833
Electrolysis PV	6.89	77	8.594
Expansion valve 1	0.02086	92	–
Expansion valve 2	1.509	99	–
Expansion valve 3	0.7748	56	–
Pump 1	124.9	39	203.7
Pump 2	10.96	3	11.35
Pump 3	0.3912	11	0.4398
Pump 4	105.4	24	138.7
Pump 5	0.1757	4	0.169
Turbine	193.1	90	1834
Compressor	0.922	55	2.042
Generator	9.943	93	–
Absorber	113.3	2	567.7
Evaporator 1	1426	58	–
Evaporator 2	2.131	95	–
Evaporator 3	0.1955	28	–
Thermal energy storage	0.9767	18	1.062
Solar PV/T	6.382	13	15.44/7.061

performed. The solar PV/T system's energy and exergy efficiencies are 23.6% and 13.3% respectively, while the power conversion efficiency of the PV/T modules is calculated to be 10.8%.

The geothermal based electrolysis process energy and exergy efficiencies are 39.1% and 32.3% respectively. About 50% of generated electricity is used in electrolysis process for hydrogen production. In geothermal based hydrogen production 18.11 kg/h hydrogen is stored in the tank. While in PV/T, 0.1185 kg/h hydrogen can be stored since the amount of produced electricity is only ca. 7 kW. PV/T based electrolysis energy efficiency is 68.2% and exergy efficiency is 77%. There is an important amount of heat loss in Heat Exchanger 1, Condenser 4 and geothermal based

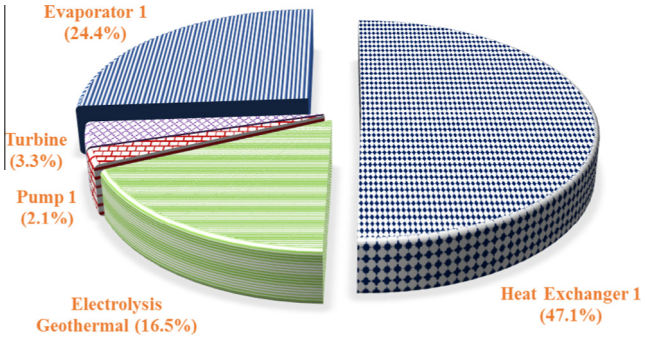

Fig. 2. Highest exergy destruction ratios for main components of the system.

electrolysis process. The produced oxygen is also stored to be transferred for medical purposes.

The overall energy and exergy efficiencies of the renewable energy based multigeneration system are calculated to be 5.5% and 20.4% respectively under given conditions at 25 °C and 100 kPa. The energetic and exergetic COPs of the absorption cooling system are found to be 0.58 and 0.17 respectively. The exergetic COP is lower than the energetic COP because there are significant losses in the absorption system especially in Absorber and Condenser 2. The energetic COP is lower than expected absorption systems because required heat input for the generator is supplied from an organic Rankine cycle whose temperature is considerably lower than conventional Rankine cycle. The energetic COP of heat pump system is 4.1 and exergetic COP is 0.03. In addition, the energy and exergy efficiencies respectively are calculated to be 16.9% and 50.3% for organic Rankine cycle. A comparison of energy and exergy efficiency values of different geothermal based co/tri/multi-generation systems, as available in the open literature, is listed in Table 5.

It is further important to mention that integrating both solar and geothermal subsystems overcomes any issues related to hourly changes in the solar radiation intensities reaching the solar collecting devices and some seasonal changes in geothermal water temperatures. It also gives a better and more reliable multigeneration opportunity to meet the demands of users.

An important advantage of exergy analysis is that it takes reference ambient conditions into account. In order to understand the effect of ambient conditions on subsystem and overall efficiencies, some parametric studies are executed. Additionally, the effect of working fluid type is studied, and the changes in efficiencies by variable working fluids are determined.

4.1. Effect of ambient pressure

When the ambient pressure increases from 80 kPa to 130 kPa which might change according to the altitude of location, although energy efficiency does not change, exergy efficiency decreases very slightly. Even though for some of the subsystems, pressure change might be more

Table 5
Energy and exergy efficiency comparison of various geothermal based systems in the literature.

Author	Energy efficiency (%)	Exergy efficiency (%)	System description
Franco and Villani (2009)	9.27	31.45	Rankine with superheater $T_{geo} = 150$ °C Isobutane
	10.89	36.98	Supercritical cycle Optimized solution R134a $T_{geo} = 150$ °C
Zhou (2014)	10.8	14.7	Supercritical hybrid solar–geothermal plant
	11.6	14.1	Subcritical hybrid solar–geothermal plant
Heberle and Brüggemann (2010)	14	53	Geothermal ORC with internal heat recovery Isobutane $T_{geo} = 160$ °C
Coskun et al. (2012)	39.9	54.8	Geothermal Domestic hot water, heating, electricity $T_{geo} = 156$ °C
Al-Ali and Dincer (2014)	78	36.6	Geothermal-solar cycle, organic Rankine cycle and single absorption chiller $T_{geo} = 190$ °C
El-Emam and Dincer (2013)	16.37	48.8	Geothermal regenerative organic Rankine cycle $T_{geo} = 175$ °C
AlZaharani et al. (2013)	13.67	32.27	Supercritical carbon dioxide (CO_2) Rankine cycle with an organic (R600) Rankine cycle, an electrolyzer, and a heat recovery system $T_{geo} = 200$ °C
Suleman et al. (2014)	54.7	76.4	Combined geothermal and solar energy system

effective, overall efficiency is not much affected by ambient pressure.

4.2. Effect of ambient temperature

Ambient temperature is critical for the performance of most thermodynamic systems. Therefore, changes in ambient temperature may increase or decrease the system efficiency. The effects of variations in ambient temperature on some of the subsystems and overall efficiency of the multigeneration system are shown in Figs. 3 and 4. By increasing ambient temperature in Figs. 3 and 4, energetic COP of both absorption cooling system and heat pump system remains constant however exergetic COP of absorption cooling system increases dramatically from 0.1 to 0.75. On the other hand, heat pump's exergetic COP is decreasing from 4.4 to 3.7 by a change of ambient temperature from 15 °C to 25 °C.

The organic Rankine cycle exergy efficiency increases up to 60% by increasing ambient temperature from 15 °C to 50 °C as shown in Fig. 4 although the turbine efficiencies remain constant. Overall multigeneration system energy efficiency remains constant with increasing ambient temperature however exergy efficiency of the system increases up to 27% at 50 °C as Fig. 4 emphasizes. It shows that the designed system will work more exergetically efficient under high temperature ambient conditions.

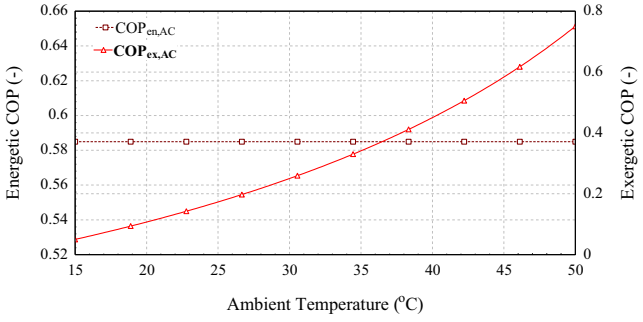

Fig. 3. Variation of absorption cooling system COPs with increasing ambient temperature.

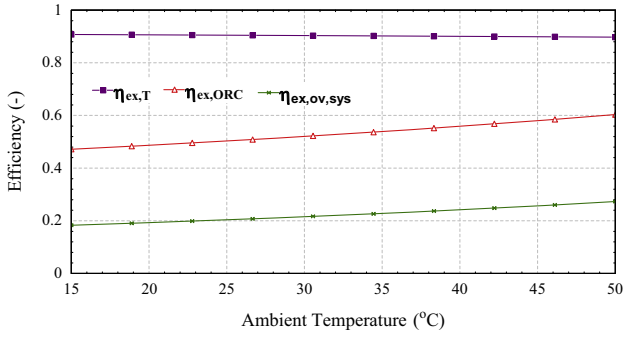

Fig. 4. Variation of turbine, organic Rankine cycle and overall system exergy efficiencies with increasing ambient temperature.

4.3. Effect of mass flow rates on some components and overall efficiencies

There are two independent inputs to the system; geothermal energy and solar energy. The mass flow rates of these systems play an important role on overall system efficiency. As seen in Fig. 5, an increase in the geothermal water mass flow rate will lower both organic Rankine cycle and overall system efficiency. This indicates us that the power output increase will be much lesser than power input increase.

Increase in water mass flow rate in solar energy system decreases both energy and exergy efficiencies of overall

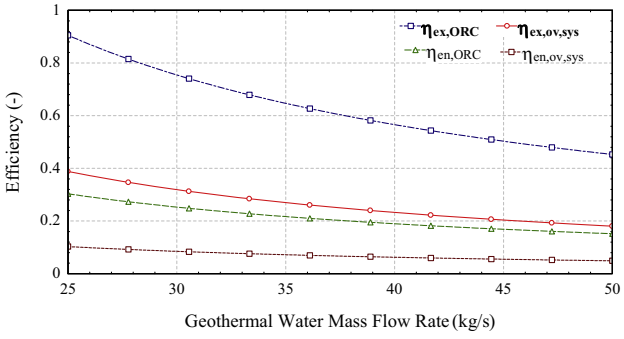

Fig. 5. Variation of organic Rankine cycle and overall energy–exergy efficiencies with changing geothermal water mass flow rate.

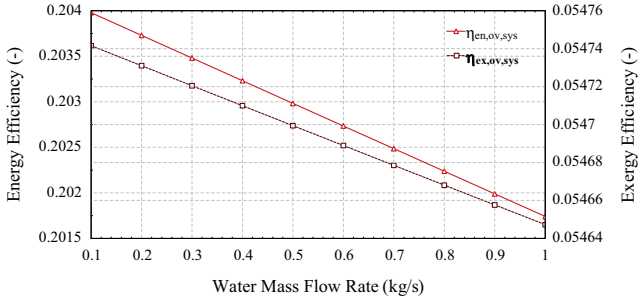

Fig. 6. Variation of overall energy and exergy efficiencies with changing water mass flow rate in Solar PV/T system.

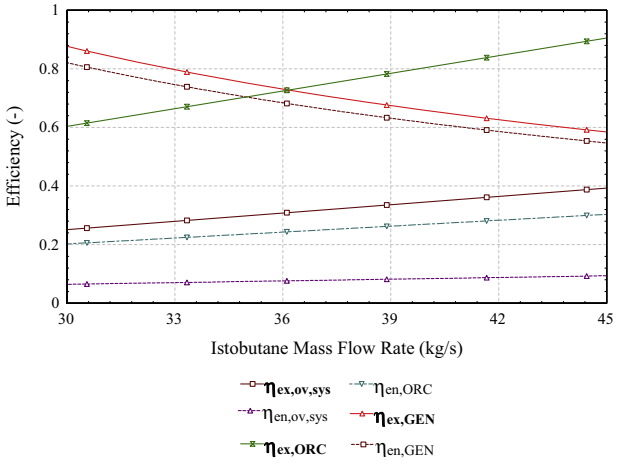

Fig. 7. Effects of working fluid isobutane mass flow rate on generator, organic Rankine cycle and overall system efficiencies.

system in Fig. 6. Because water mass flow rate in solar energy system is one of the two inputs of the overall system. Overall exergy efficiency decreases down to 20.1% from 20.4%. Rising the isobutane mass flow rate in the organic Rankine cycle decreases the generator efficiencies in Fig. 7 because generator's input is the output of turbine. This will increase denominator of efficiency definition of generator. On the other hand, increasing isobutane mass flow rate in organic Rankine cycle, rises both organic Rankine cycle and overall efficiencies. The exergy efficiency of organic Rankine cycle increases up to 90% and overall system efficiency increases up to 40% at 45 kg/s mass flow rate.

4.4. Effect of global solar irradiance on solar energy system and overall efficiencies

Fig. 8 indicates that increasing solar irradiance decreases both energy and exergy efficiency of solar energy system because energy output of solar module increases less than increase in solar irradiance. Since average solar irradiance in Arabic countries and Mediterranean region changes between 600 W/m^2 and 1000 W/m^2 during seasons, energy efficiency goes down to 19% from 32% by increasing solar irradiance. The exergy efficiency of solar energy system decreases to 10% at 1000 W/m^2 solar irradiance. The overall system performance is not affected by solar irradiance change.

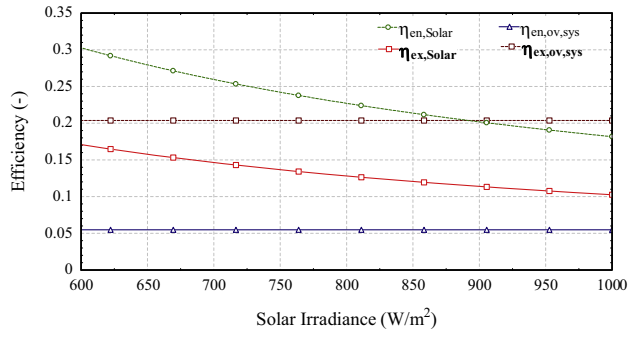

Fig. 8. Effects of global solar irradiance on solar PV/T system and overall efficiencies.

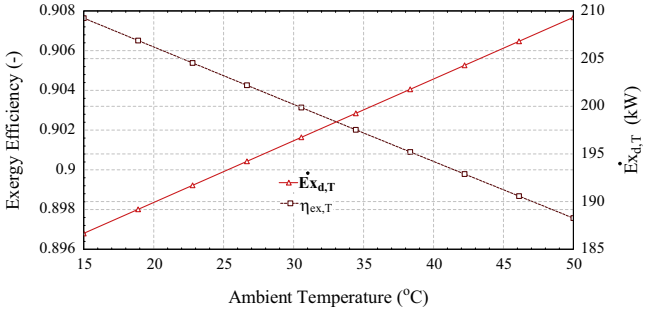

Fig. 9. Change of turbine exergy destruction rate and exergy efficiency with varying ambient temperature.

4.5. Change of exergy destruction rate and exergy efficiency by changing ambient temperature

Figs. 9 and 10 indicate that exergy destruction rates of components are inversely proportional with exergy efficiencies by increasing ambient temperature. As seen in Fig. 9, when the turbine exergy destruction rate increases from 185 kW to 210 kW by an increment of 35 °C ambient temperature, exergy efficiency of Turbine decreases more than 1%. The compressor exergy destruction rate is also reverse proportional with exergy efficiency when the temperature increases from 15 °C to 50 °C even though the change is around 4%. The solar PV/T system exergy efficiency decreases to 12.5% from 13.5% by an increasing temperature and exergy destruction rate. Another high exergy destruction rate is observed in Evaporator 1. As seen in Fig. 10, the exergy efficiency of Evaporator 1 decreases to 42% with increasing ambient temperature and exergy destruction rate.

4.6. Effect of working fluid on organic Rankine cycle and overall system

The working fluid type used in organic Rankine cycle efficiency is an important factor on system efficiencies. A parametric study is carried out by defining three different type of working fluids: isobutane, R123 and R245fa. As seen in Figs. 11 and 12, highest exergy efficiency in organic

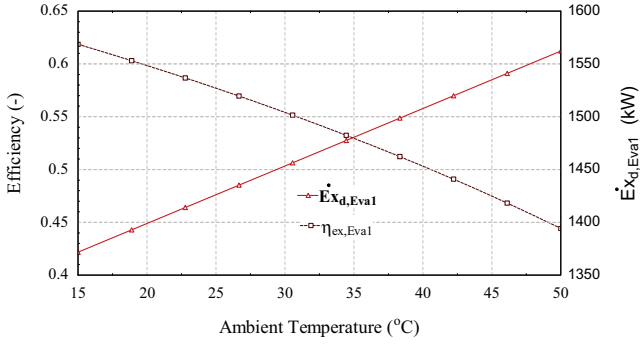

Fig. 10. Change of Evaporator 1 exergy destruction rate and exergy efficiency with varying ambient temperature.

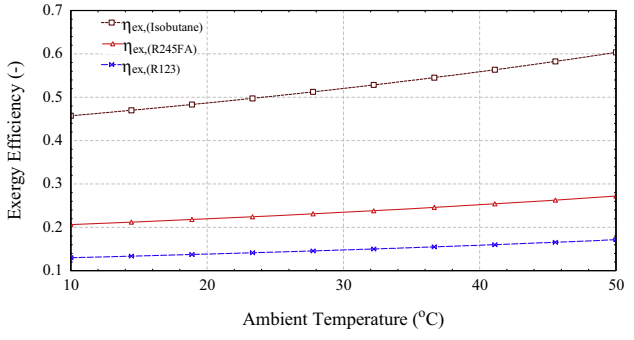

Fig. 11. Effects of working fluid type with varying ambient temperature on exergy efficiency of organic Rankine cycle.

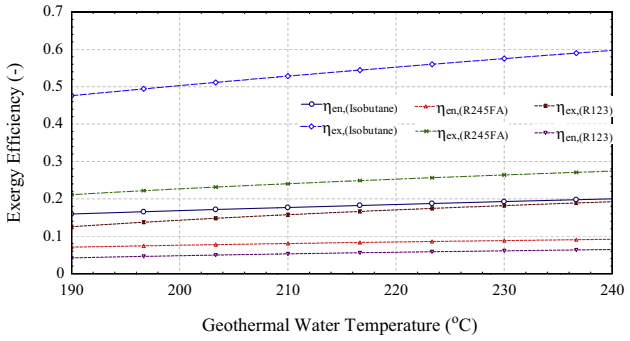

Fig. 12. Working fluid effect with varying geothermal temperature on energy and exergy efficiencies of organic Rankine cycle.

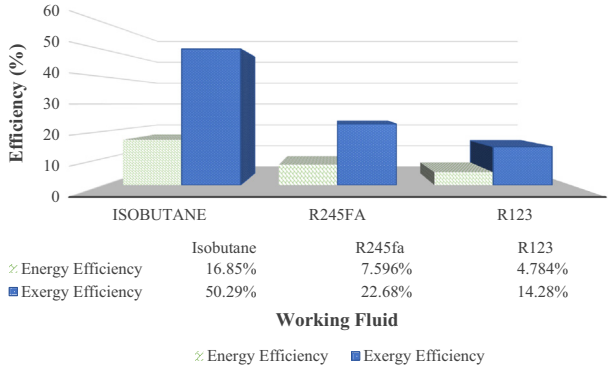

	Isobutane	R245fa	R123
Energy Efficiency	16.85%	7.596%	4.784%
Exergy Efficiency	50.29%	22.68%	14.28%

Fig. 13. Comparison of energy and exergy efficiency values of organic Rankine cycle under different type of working fluids at 25 °C and 100 kPa ambient conditions.

Rankine cycle is observed when isobutane is used in organic Rankine cycle. At 25 °C ambient temperature, exergy efficiency is 50% although it is about 22% and 13% for R254fa and R123 respectively. This proves that system is approximately 3 times more efficient when isobutane is used.

Another parametric study related to geothermal water temperature and working fluid indicates that when the geothermal water temperature increases up to 240 °C, all efficiencies are increasing however highest increase is still in isobutane which corresponds to 60% organic Rankine cycle exergy efficiency at 240 °C. The system is more efficient when R245fa is used than R123 as seen in Fig. 12. A comparison of efficiency values for three type of working fluid is seen in Figs. 13 and 14 under same values and ambient conditions. Evaporator 1 has highest exergy destruction rate when R123 working fluid is used. Since absorption cooling system is integrated with organic Rankine cycle turbine output, Evaporator 2 heat input which is in fact cooling effect decreases to 223.9 kW and 176.3 kW when R245fa and R123 is used respectively.

4.7. Effect of geothermal water temperature on overall system

The main input to the electrolysis of water is power. When the power input increases, more water is split and

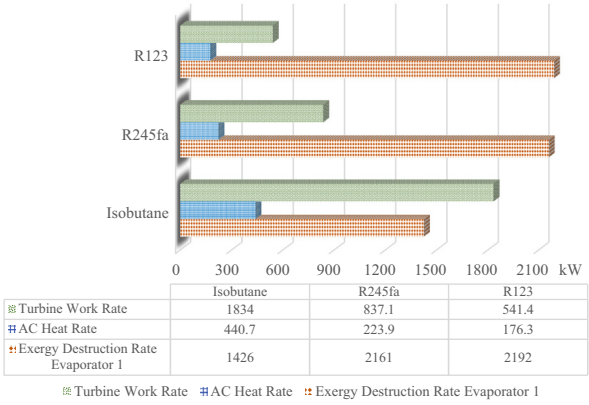

	Isobutane	R245fa	R123
Turbine Work Rate	1834	837.1	541.4
AC Heat Rate	440.7	223.9	176.3
Exergy Destruction Rate Evaporator 1	1426	2161	2192

Turbine Work Rate AC Heat Rate Exergy Destruction Rate Evaporator 1

Fig. 14. Working fluid effect on work/heat rates and exergy destruction rates (kW) related to organic Rankine cycle.

more hydrogen is produced. In geothermal based hydrogen production, the power is supplied by turbine–generator output. Since the power output increases when the geothermal water temperature rises, the amount of hydrogen produced by the system increases in parallel. If the geothermal water temperature is 220 °C, the stored hydrogen increases to around 20 kg in hour. Similarly, the PV based hydrogen production is much higher when generated PV power is higher. It reaches to 0.16 kg/h when twelve more PV/T modules are used as illustrated in Fig. 15.

The geothermal water temperature directly influences the total turbine work output and absorption cooling system as seen in Fig. 16. The generated work increases to

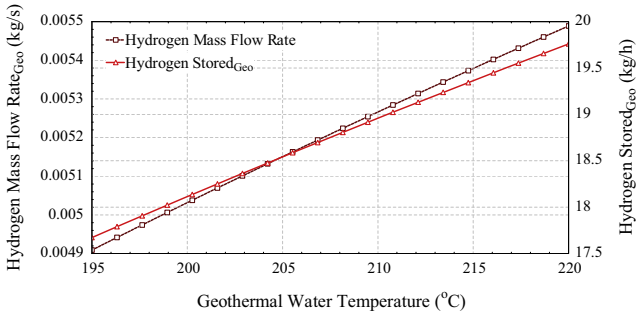

Fig. 15. Effects of geothermal water temperature on hydrogen production.

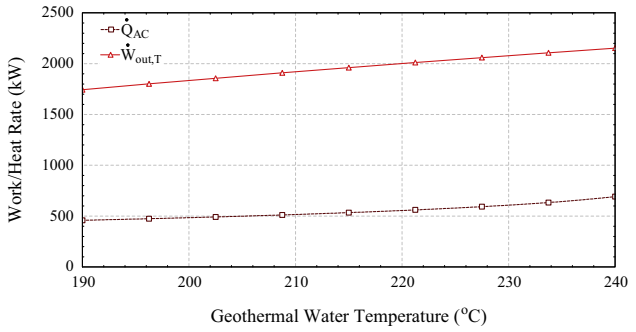

Fig. 16. Effects of geothermal water temperature on turbine work output and absorption cooling heat rate.

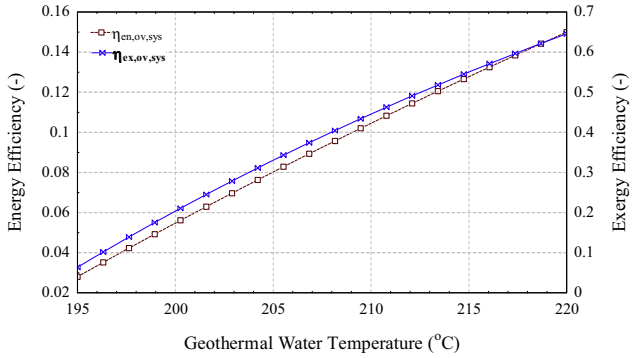

Fig. 17. Variation of overall energy and exergy efficiencies with increasing geothermal water temperature.

2.1 MW and cooling effect to 700 kW when geothermal water temperature is 240 °C. The overall system efficiencies are strictly dependent on geothermal water temperature as stated in Fig. 17. In case we have higher geothermal water temperature such as 220 °C, the energy efficiency of multigeneration system can increase up to 15% and exergy efficiency up to 65%. Therefore, the overall system will work more efficient on a high temperature geothermal zone. The exergy results show that organic Rankine cycle evaporator and Heat Exchanger 1 are the two main sources of irreversibility, with the largest exergy destruction rate due to the high mass flow rate of geothermal water input and high temperature difference in both components. In addition, the geothermal based electrolysis has the third highest exergy destruction rate with a value of 961.4 kW. The proposed multigeneration system efficiencies can be compared with the ones in the literature. Heberle and Brüggemann (2010) showed an exergy efficiency of 35–40% for the multigeneration system combining solar and geothermal energy. Suleman et al. (2014) found the exergy efficiency ranging between 60% and 70% for solar collector and geothermal based multigeneration system. (Karellas and Braimakis, 2016) used biomass and solar energy for multigeneration. But their organic Rankine cycle efficiency was about 7% which is low compared the current study. Ayub et al. (2015) proposed integration of geothermal and solar energy. The exergy efficiency changes between 39% and 42% depending on the mass flow rate. In the current study, it ranges between 20% and 40% depending on the mass flow rate. In Dağdaş et al. (2005), the energy and exergy efficiencies of sole geothermal based power plant can be seen under various conditions. The energy and exergy efficiencies were about 8% and 38%, respectively. In the current study, both efficiencies are higher than using only geothermal plant or sole solar energy. Therefore, combining various renewable resources in a clean and environmentally benign manner would bring both higher efficiencies and better sustainability. The results of this study are encouraging for solar and geothermal based hybrid system which shows a good opportunity for low cost electricity production and higher efficiency combined system by increasing the attractiveness of many low-medium temperature geothermal sources.

5. Conclusions

In this paper, a novel renewable energy based multigeneration system together with hydrogen production is designed and analyzed for heating, cooling, hot water, electricity and hydrogen production. The electricity production is achieved by geothermal based organic Rankine cycle and solar PV/T modules. Absorption cooling system is based on organic Rankine cycle turbine output. Solar PV/T modules are the driven source of thermal energy storage and heat pump system. By a duct system under solar PV/T modules, required water for electrolysis is conditioned in order to increase the water temperature.

The effects of certain operating conditions on the subsystems and overall system performance are investigated. Extensive parametric studies on the efficiencies under various ambient temperature, pressure and mass flow rate values are examined and results are comparatively discussed. Any change in ambient pressure has not an important effect on overall efficiency as well as organic Rankine cycle efficiency. Increasing ambient temperature of the system positively influences exergetic COP of absorption cooling, exergy efficiency of organic Rankine cycle, PV based electrolysis process and overall system. The overall system exergy efficiency increases to 27% at the ambient temperature of 50 °C. In addition, geothermal water temperature is directly increasing the overall system efficiency up to 60% when water temperature is 220 °C. An increase of 25 °C in geothermal water temperature from 195 °C to 225 °C, raises energy efficiency of multigeneration system up to 15%.

In summary, highest energy and exergy efficiencies are calculated as 15% and 65% respectively when geothermal water temperature is 220 °C. Compared to second law analysis, the first law analysis takes into account the thermal energy of geothermal water, which is actually transferred to the ORC instead of the potentially available thermal energy of geothermal water hence yielding higher exergy efficiency. The evaporator 1, turbine and pump 4 in organic Rankine cycle have high exergy destruction rates as components, accounting for about 30% of the total exergy destruction rates of the overall system. In geothermal based hydrogen production system, 18 kg and in PV/T based hydrogen production system 0.11 kg hydrogen can be stored per hour. Additionally, it is seen that under given conditions, isobutane is the best alternative as working fluid of organic Rankine cycle while decreasing the exergy destructions and increasing the turbine work output. As a result, the renewable energy based hybrid multi generation systems together with hydrogen production for different type of commodities can be used for various applications, such as stand-alone factories, houses and dairy farms.

Acknowledgement

The authors acknowledge the support provided by the Natural Sciences and Engineering Research Council of Canada.

References

Acar, C., Dincer, I., 2014. Comparative assessment of hydrogen production methods from renewable and non-renewable sources. Int. J. Hydrogen Energy 39 (1), 1–12.

Ahmadi, P., Dincer, I., Rosen, M.A., 2013. Development and assessment of an integrated biomass-based multi-generation energy system. Energy 56, 155–166.

Al-Ali, M., Dincer, I., 2014. Energetic and exergetic studies of a multigenerational solar–geothermal system. Appl. Therm. Eng. 71 (1), 16–23.

Al-Sulaiman, F.A., Dincer, I., Hamdullahpur, F., 2011. Exergy modeling of a new solar driven trigeneration system. Sol. Energy 85 (9), 2228–2243.

AlZaharani, A.A., Dincer, I., Naterer, G.F., 2013. Performance evaluation of a geothermal based integrated system for power, hydrogen and heat generation. Int. J. Hydrogen Energy 38 (34), 14505–14511.

Artuso, P., Gammon, R., Orecchini, F., Watson, S.J., 2011. Alkaline electrolysers: model and real data analysis. Int. J. Hydrogen Energy 36 (13), 7956–7962.

Astolfi, M., Xodo, L., Romano, M.C., Macchi, E., 2011. Technical and economical analysis of a solar–geothermal hybrid plant based on an Organic Rankine Cycle. Geothermics 40 (1), 58–68.

Ayub, M., Mitsos, A., Ghasemi, H., 2015. Thermo-economic analysis of a hybrid solar-binary geothermal power plant. Energy 87, 326–335.

Balta, M.T., Dincer, I., Hepbasli, A., 2009. Thermodynamic assessment of geothermal energy use in hydrogen production. Int. J. Hydrogen Energy 34 (7), 2925–2939.

Balta, M.T., Dincer, I., Hepbasli, A., 2010. Geothermal-based hydrogen production using thermochemical and hybrid cycles: a review and analysis. Int. J. Energy Res. 34 (9), 757–775.

Barbir, F., 2005. PEM electrolysis for production of hydrogen from renewable energy sources. Sol. Energy 78 (5), 661–669.

Bertani, R., 2012. Geothermal power generation in the world 2005–2010 update report. Geothermics 41, 1–29.

Bouzguenda, M., 2012. A comparative study of hybrid diesel solar PV–wind power systems in rural areas in the Sultanate of Oman. Int. J. Sustain. Energ. 31 (2), 95–106.

Carmo, M., Fritz, D.L., Mergel, J., Stolten, D., 2013. A comprehensive review on PEM water electrolysis. Int. J. Hydrogen Energy 38 (12), 4901–4934.

Cengel, Y.A., Boles, M.A., 2014. Thermodynamics: An Engineering Approach, eighth ed. McGraw-Hill, New York, USA.

Chamorro, C.R., Mondéjar, M.E., Ramos, R., Segovia, J.J., Martín, M. C., Villamañán, M.A., 2012. World geothermal power production status: energy, environmental and economic study of high enthalpy technologies. Energy 42 (1), 10–18.

Cho, H., Smith, A.D., Mago, P., 2014. Combined cooling, heating and power: a review of performance improvement and optimization. Appl. Energy 136, 168–185.

Coskun, C., Oktay, Z., Dincer, I., 2012. Thermodynamic analyses and case studies of geothermal based multi-generation systems. J. Cleaner Prod. 32, 71–80.

Dağdaş, A., Öztürk, R., Bekdemir, Ş., 2005. Thermodynamic evaluation of Denizli K±z±ldere geothermal power plant and its performance improvement. Energy Convers. Manage. 46 (2), 245–256.

Dincer, I., 2012. Green methods for hydrogen production. Int. J. Hydrogen Energy 37 (2), 1954–1971.

Dincer, I., Rosen, M.A., 2013. Exergy, Energy, Environment and Sustainable Development, second ed. Elsevier, New York, USA.

Dincer, C., Zamfirescu, C., 2011. Sustainable Energy Systems and Applications. Springer Science+Business Media, LLC.

Dincer, I., Zamfirescu, C., 2012. Renewable-energy-based multigeneration systems. Int. J. Energy Res. 36, 1403–1415.

El-Emam, R.S., Dincer, I., 2013. Exergy and exergoeconomic analyses and optimization of geothermal organic Rankine cycle. Appl. Therm. Eng. 59 (1–2), 435–444.

Ferrero, D., Lanzini, A., Santarelli, M., Leone, P., 2013. A comparative assessment on hydrogen production from low- and high-temperature electrolysis. Int. J. Hydrogen Energy 38 (9), 3523–3536.

Franco, A., Villani, M., 2009. Optimal design of binary cycle power plants for water-dominated, medium-temperature geothermal fields. Geothermics 38 (4), 379–391.

Guo, T., Wang, H., Zhang, S., 2011. Comparative analysis of natural and conventional working fluids for use in transcritical Rankine cycle using low-temperature geothermal source. Int. J. Energy Res. 35, 530–544.

Hand, T.W., 2008. Hydrogen Production Using Geothermal Energy [M. S.]. Utah State University, Ann Arbor.

Heberle, F., Brüggemann, D., 2010. Exergy based fluid selection for a geothermal Organic Rankine Cycle for combined heat and power generation. Appl. Therm. Eng. 30 (11–12), 1326–1332.

Joshi, A.S., Dincer, I., Reddy, B.V., 2009. Thermodynamic assessment of photovoltaic systems. Sol. Energy 83 (8), 1139–1149.

Kalogirou, S.A., Karellas, S., Badescu, V., Braimakis, K., 2016. Exergy analysis on solar thermal systems: a better understanding of their sustainability. Renewable Energy.

Karellas, S., Braimakis, K., 2016. Energy–exergy analysis and economic investigation of a cogeneration and trigeneration ORC–VCC hybrid system utilizing biomass fuel and solar power. Energy Convers. Manage. 107, 103–113.

Khalid, F., Dincer, I., Rosen, M.A., 2015. Energy and exergy analyses of a solar-biomass integrated cycle for multigeneration. Sol. Energy 112, 290–299.

Kumar, A., Kumar, R., 2014. Thermodynamic analysis of a novel compact power generation and waste heat operated absorption, ejector-jet pump refrigeration cycle. J. Mech. Sci. Technol. 28 (9), 3895–3902.

Moran, M.J., Shapiro, H.N., Boettner, D.D., Bailey, M.B., 2011. Fundamentals of Engineering Thermodynamics, seventh ed. Wiley.

Nieminen, J., Dincer, I., Naterer, G., 2010. Comparative performance analysis of PEM and solid oxide steam electrolysers. Int. J. Hydrogen Energy 35 (20), 10842–10850.

Ozcan, H., Dincer, I., 2014. Energy and exergy analyses of a solar driven Mg–Cl hybrid thermochemical cycle for co-production of power and hydrogen. Int. J. Hydrogen Energy 39 (28), 15330–15341.

Ozturk, M., Dincer, I., 2013a. Thermodynamic analysis of a solar-based multi-generation system with hydrogen production. Appl. Therm. Eng. 51 (1–2), 1235–1244.

Ozturk, M., Dincer, I., 2013b. Thermodynamic assessment of an integrated solar power tower and coal gasification system for multi-generation purposes. Energy Convers. Manage. 76, 1061–1072.

Ratlamwala, T.A.H., Gadalla, M.A., Dincer, I., 2011. Performance assessment of an integrated PV/T and triple effect cooling system for hydrogen and cooling production. Int. J. Hydrogen Energy 36 (17), 11282–11291.

Roy, A., Watson, S., Infield, D., 2006. Comparison of electrical energy efficiency of atmospheric and high-pressure electrolysers. Int. J. Hydrogen Energy 31 (14), 1964–1979.

Sahin, A.D., Dincer, I., Rosen, M.A., 2007. Thermodynamic analysis of solar photovoltaic cell systems. Sol. Energy Mater. Sol. Cells 91 (2–3), 153–159.

Suleman, F., Dincer, I., Agelin-Chaab, M., 2014. Development of an integrated renewable energy system for multigeneration. Energy 78, 196–204.

The Exergoecology Portal. <http://www.exergoecology.com/excalc/> (accessed 21.12.2014).

Tunc, M., Sisbot, S., Camdali, U., 2013. Exergy analysis of electricity generation for the geothermal resources using organic rankine cycle: K±z±ldere-denizli case. Environ. Progr. Sustain. Energy 32 (3), 830–836.

Turkish State Meteorological Service. <http://www.mgm.gov.tr/veride-gerlendirme/il-ve-ilceler-istatistik.aspx> (accessed 07.08.2015).

VOLTHER PowerTherm&PowerVolt, 2014. <http://www.solimpeks.com/wp-content/uploads/2012/12/Volther-Datasheet.pdf> (accessed 01.12.2014).

Wang, X.D., Zhao, L., Wang, J.L., Zhang, W.Z., Zhao, X.Z., Wu, W., 2010. Performance evaluation of a low-temperature solar Rankine cycle system utilizing R245fa. Sol. Energy 84 (3), 353–364.

Yekoladio, P.J., Bello-Ochende, T., Meyer, J.P., 2015. Thermodynamic analysis and performance optimization of organic rankine cycles for the conversion of low-to-moderate grade geothermal heat. Int. J. Energy Res. 39, 1256–1271.

Yilanci, A., Dincer, I., Ozturk, H.K., 2009. A review on solar-hydrogen/fuel cell hybrid energy systems for stationary applications. Prog. Energy Combust. Sci. 35 (3), 231–244.

Zhang, N., Lior, N., 2006. Development of a novel combined absorption cycle for power generation and refrigeration. J. Energy Res. Technol. 129 (3), 254–265.

Zhou, C., 2014. Hybridisation of solar and geothermal energy in both subcritical and supercritical Organic Rankine Cycles. Energy Convers. Manage. 81, 72–82.